Effects of natural starch-phosphate monoester content on the multi-scale structures of potato starches

Li Ding [a],[1], Wenxin Liang [a],[1], Jianzhou Qu [b], Staffan Persson [a],[c], Xingxun Liu [d],[e],[f], Klaus Herburger [a],[j], Jacob Judas Kain Kirkensgaard [g],[i], Bekzod Khakimov [g], Kasper Enemark-Rasmussen [h], Andreas Blennow [a],[*], Yuyue Zhong [a],[*]

[a] Copenhagen Plant Science Center, Department of Plant and Environmental Sciences, Faculty of Science, University of Copenhagen, Denmark
[b] Key Laboratory of Biology and Genetic Improvement of Maize in Arid Area of Northwest Region, Ministry of Agriculture, College of Agronomy, Northwest A&F University, Yangling, Shaanxi, China
[c] Joint International Research Laboratory of Metabolic & Developmental Sciences, State Key Laboratory of Hybrid Rice, SJTU-University of Adelaide Joint Centre for Agriculture and Health, School of Life Sciences and Biotechnology, Shanghai Jiao Tong University, Shanghai, China
[d] Lab of Food Soft Matter Structure and Advanced Manufacturing, College of Food Science and Engineering, Nanjing University of Finance and Economics, Nanjing 210023, China
[e] Collaborative Innovation Center for Modern Grain Circulation and Safety, Nanjing University of Finance and Economics, Nanjing 210023, China
[f] Key Laboratory of Grains and Oils Quality Control and Processing, Nanjing University of Finance and Economics, Nanjing 210023, China
[g] Department of Food Science, University of Copenhagen, DK-1958 Frederiksberg C, Denmark
[h] Department of Chemistry, Technical University of Denmark, Kemitorvet, Building 207, DK-2800 Kgs. Lyngby, Denmark
[i] Niels Bohr Institute, University of Copenhagen, DK-2100 Copenhagen Ø, Denmark
[j] Institute of Biological Sciences, University of Rostock, Rostock, Germany

ARTICLE INFO

ABSTRACT

Starch phosphate content (SPC) is an important structural parameter affecting the functionality of tuber starches, but how different phosphate groups affect starch structures is still unknown. In this study, four potato starches with different SPC were selected as models to investigate the effects of SPC on their multi-scale structures. A higher SPC is related to more long amylopectin (AP) chains with a degree of polymerization (DP) >24, fewer short AP chains with DP $\leq$ 24, lower double helical content and crystallinity, higher long period distance, and lower scattering intensity (I_{max}), indicating that potato starch with a higher SPC is less ordered and has a more flexible nano-lamellar structure. Notably, two types of phosphate monoesters, namely C-3 (C3P) and C-6 phosphate monoesters (C6P), were both significantly positively correlated with the average chain lengths (ACL) of AP chains with DP 25–36 (fb2) and negatively correlated with I_{max}; however, only C3P was significantly positively correlated with ACL of AP chains with DP 13–24 (fb1) and negatively correlated with the absorbance ratio at 1047/1016 cm^{-1}. C3P was the main reason for the disordered structure of starches with high SPC. These findings can be helpful for potato breeding to generate different functionality by controlling SPC.

Table 1
Sample code, phosphate and amylose contents of potato and maize starch samples.

Starch varieties	Sample code	SPC (nmol/mg starch)	C3P (nmol/mg starch)	C6P (nmol/mg starch)	AC (%)	References[a]
Waxy potato (Kuras)	WPS	25.0	3.7	21.3	1.9	(Kozlov et al., 2007; Wikman, Blennow, & Bertoft, 2013)
Normal potato (Dianella)	NPS	24.0	9.9	14.1	19.8	(Kozlov et al., 2007; Wikman et al., 2013)
Low phosphate potato (asGWD)	LPPS	3.1	0.9	2.2	28.2	(Wikman et al., 2011)
High phosphate potato (asSBE)	HPPS	73.8	21.8	52.0	29.6	(Wikman et al., 2011)
Waxy maize	WMS	n.d.[b]	n.d.	n.d.	0.05	(Zhong, Tian, et al., 2021)
Normal maize	NMS	n.d.	n.d.	n.d.	30.7	(Zhong, Keeratiburana, et al., 2021)

[a] The starch phosphate content (SPC), C-3 phosphate monoester content (C3P), and C-6 phosphate monoester content (C6P) in the four potato starches are referred from previous data. The amylose content (AC) was analyzed by the iodine complexation method (Carciofi et al., 2012).

[b] n.d = not detectable.

1. Introduction

Potato (*Solanum tuberosum* L.) is one of the most important staple crops worldwide and plays a significant role in global food security (Blennow et al., 2020). Starch is the major component in potato tubers, accounting for 70–90 % of the dry mass (Nayak, Berrios, & Tang, 2014). Starch granules have a semi-crystalline granular structure, which is molecularly composed of two types of α-glucans, mostly unbranched amylose (AM) and highly branched amylopectin (AP). The AM content (AC) of normal potato starches ranges typically from 15 % to 30 % (Karlsson, Leeman, Björck, & Eliasson, 2007; Liu, Tarn, Lynch, & Skjodt, 2007). The AC has been well known to determine the multi-scale structure of starch granules, thereby governing the functionality of the starch, e.g., its viscosity, texture, and digestibility (Cai, Zhao, Huang, Chen, & Wei, 2014; Li, Dhital, Flanagan, et al., 2020; Lin, Guo, Zhao, et al., 2016; Zhong, Liu, et al., 2020) and the performance of starch-based products (Han et al., 2017). For example, a higher AC is associated with a lower AM molecular size and a higher proportion of long AP chains in maize and wheat starches (Li, Dhital, Gilbert, & Gidley, 2020; Zhong, Liu, et al., 2020), a lower small angle X-ray scattering (SAXS) Bragg nano-lamellar repeat distance in maize starch (Zhong, Liu, et al., 2020), lower SAXS peak scattering intensity in potato starch (Kozlov, Blennow, Krivandin, & Yuryev, 2007) and a lower starch crystallinity in sweet potato (Zhou et al., 2015) and rice (Zhong, Li, et al., 2021).

In addition to the AC, phosphorylation of the AP molecules is another key factor affecting the functionality of root and tuber starches (Blennow & Engelsen, 2010). Potato starch naturally contains one of the largest quantities of phosphate monoesters, with starch phosphate contents (SPC) ranging from 30.8 to 124.4 mg/100 g (Noda et al., 2007). Phosphorylation of the C-6 positions of the glucosyl units (C6P), catalyzed by the glucan water dikinase 1 (GWD1), represents the majority (60–70 %) of the phosphate groups in starch. The remaining phosphate groups are generated from C-3 phosphorylation (C3P), catalyzed by the glucan water dikinase 3/phosphoglucan water dikinase (GWD3/PWD) (Wikman et al., 2011; Xu, Huang, Visser, & Trindade, 2017). The unique quality of potato starch pastes, such as high paste clarity and viscosity, is attributed to these phosphate monoesters, which provide native starch granules with highly hydrated local cavities (Wikman et al., 2011). In addition, potato starches with higher SPC show a higher swelling power, peak viscosity, breakdown values (Noda et al., 2007), and reduced enzymatic digestibility (Wickramasinghe, Blennow, & Noda, 2009). Hence, the content of phosphate monoesters is an important structural parameter affecting the functionality of potato starches. However, how precisely phosphate groups affect the multi-scale structures is unknown, mainly due to the limited potato sources with SPC variations.

Over two decades, our lab has engineered a high SPC potato mutant by using dual RNA interference antisense (RNAi) suppression of starch branching enzyme I and II (asSBE) (Blennow et al., 2005), and a low SPC potato mutant by RNAi suppression of GWD1 (asGWD) (Kozlov et al.,

2007). The SBE suppressor lines revealed that longer AP chains (DP > 20) resulted in a higher SPC, higher gelatinization temperatures, and a stronger elastic gel (Blennow et al., 2005; Wikman et al., 2011). GWD1 suppressor lines produced starch with an increased AC and reduced viscosity (Viksø-Nielsen et al., 2001). However, how SPC affects the multi-structures of starches, such as helical, crystalline, and lamellar structures, remains to be investigated, which limits the understanding of the relationship between structure and functionality of phosphorylated starch types. In addition, a better understanding of how phosphate content and distribution affect multi-scale structures will permit future customization of elite potato lines with desirable functionality by new breeding technologies. Few studies have been reported that C6P is preferentially located in the amorphous regions of the starch granules, whereas C3P is equally distributed among the semi-crystalline and amorphous regions (Blennow, Bay-Smidt, Olsen, & Møller, 2000; Engelsen et al., 2003). Force-field modeling further indicated that the C6P units might fit into a natural void in the double helices of amylopectin without inflicting steric problems, while C3P might exert a significant strain or make local defects in the crystalline AP sections by inducing a major shift in the conformational equilibrium of the glucosidic linkage, thereby destabilizing the helical structure (Hansen et al., 2009). Therefore, we hypothesized that C3P and C6P have different functionality on multi-scale structures of starches, and they are as important as AC in affecting starch structures.

To reveal how SPC affects the multi-scale structures of starch and to test whether the C3P and C6P have different functionality on starch structures, four native types of potato starches with different SPC (3–74 nmol/mg starch), C3P (1–22 nmol/mg starch) and C6P (2–52 nmol/mg starch) were selected as model systems. As these four starches also contain 2–30 % of AC, two types of non-phosphorylated maize starch with different AC (0.1 % and 30.5 %) were used as controls to test whether this parameter exert specific functionalities related to phosphorylated starch systems. The multi-scale structures of these six types of starches were analyzed, including their molecular, helical, crystalline, lamellar, and granular structures, and the relationships between the phosphate contents (SPC, C3P and C6P) and multi-scale structural parameters were then discussed using principal component and Pearson correlation analysis. The findings of this study will fill the knowledge gaps on how different phosphate monoesters, i.e., C3P and C6P, affect the starch multi-scale structures and provide a foundation for breeding and engineering elite potato varieties with desirable functionality by controlling phosphate groups.

2. Materials and methods

2.1. Materials

Four potato tuber and two maize kernel starches with different SPC and AC were selected (Table 1). The four potato starches were extracted
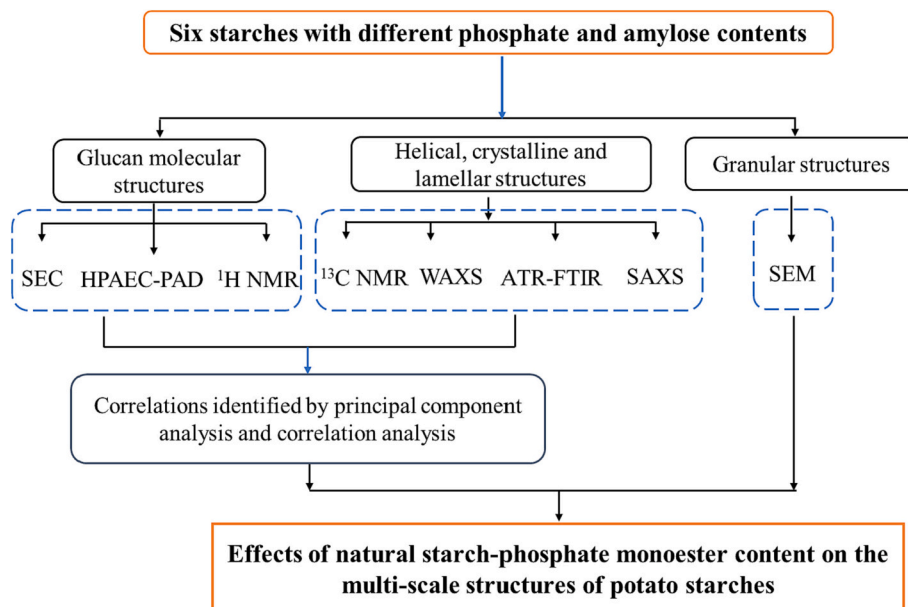
Fig. 1. Flow diagram of the experimental design.

from Dianella wild type (normal potato starch, NPS), Dianella RNAi GWD1 line (asGWD, low phosphate potato starch, LPPS), Dianella dual RNAi starch branching enzyme I and II line (asSBE, high phosphate potato starch, HPPS), and Kuras RNAi GBSS line (waxy potato starch, WPS) as described before (Blennow et al., 2005; Kozlov et al., 2007). Isoamylase (EC 3.2.1.68, E-ISAMY, 200 units/mL) and pullulanase (E-PULBL, 1000 units/mL) were bought from Megazyme (K-TSTA, Megazyme, Co. Wicklow, Ireland). All other chemicals used in this study were of analytical grade.

2.2. Size-exclusion chromatography (SEC)

Chain length distributions of debranched starch samples were analyzed using a size exclusion chromatography (SEC)-triple detector array (SEC-TDA) system (Viscotek, Malvern, UK), as previously described (Zhong, Keeratiburana, et al., 2021). The SEC was equipped with tandem GS-520HQ/GS-320HQ Shodex columns attached to a TDA302 detector array. The detailed method is described in the supplemental information.

2.3. High-performance anion exchange chromatography-pulsed amperometric detection (HPAEC-PAD)

Debranched starch samples were prepared as described in the Section 2.2 and references therein and analyzed using an HPAEC-PAD system (Dionex, Sunnyvale, CA, USA). A 40 μL of samples (5 mg/mL) was injected into a CarboPac PA-200 column at a flow rate of 0.4 mL/min. The chain length, defined as the degree of polymerization (DP) between 1 and 83, was integrated, and the detector response was corrected (Blennow, Bay-Smidt, Wischmann, Olsen, & Møller, 1998).

2.4. Solid-state ^{13}C nuclear magnetic resonance (NMR) spectroscopy

^{13}C NMR spectroscopy was performed at a ^{13}C frequency of 150.9 MHz using a Bruker AV-600 spectrometer as previously described with slight modifications (Tan, Flanagan, Halley, Whittaker, & Gidley, 2007; Zhong, Li, et al., 2021). The detailed method is described in the supplemental information. The raw NMR spectra were resolved into amorphous and ordered sub-spectra by subtracting the spectra of amorphous references at about 85 ppm, and the individual peaks in the ordered sub-spectra were fitted using Topspin software. The single and double helices are found at 102–103 ppm and 99–101 ppm, respectively, in the C1 region of ordered NMR sub-spectra, so the ratios of the peak area for single helix and double helix to the total areas are relative contents of single and double helix, respectively, and the relative content of the amorphous region was calculated by the subtraction of total relative contents of single and double helix helices from 100 % (Tan et al., 2007).

2.5. Proton nuclear magnetic resonance (^{1}H NMR) spectroscopy

The degree of branching of starch was determined using one dimensional ^{1}H NMR spectra acquired on 600 MHz NMR spectrometers (Bruker Avance III; Bruker Biospin, Rheinstetten, Germany), following a previous protocol (Zhong, Keeratiburana, et al., 2021) with some modifications. The detailed method is described in the supplemental information.

2.6. Small-angle X-ray scattering (SAXS)

SAXS was performed at the Shanghai synchrotron facility as described before (Kuang et al., 2017). Normalized 1D correlation function and SAXS scattering curve fitting were adopted to obtain a series of SAXS parameters, including Bragg lamellar repeat distance (D), peak scattering intensity (I_{max}), thickness of crystalline (d_c), amorphous lamellae (d_a) and long period distance (d_{ac}) (Xu, Blennow, Li, Chen, & Liu, 2020).

2.7. Wide-angle X-ray scattering (WAXS)

A Nano-inXider instrument (Xenocs SAS, Grenoble, France) equipped with a Cu Kα source with a 1.54 Å wavelength and a two-detector setup was used to analyze the crystalline granule structures (Zhong, Li, et al., 2021). Briefly, samples equilibrated at ~90 % relative humidity were sealed in 5–7 μm mica films and then analyzed. The radially averaged intensity I was given as a function of the scattering angle 2θ in the angular range of 5°–35° after subtraction from the mica background. The total relative crystallinity was calculated as the ratio of the crystalline peak area to the total diffraction area using PeakFit software (Version 4.0, Systat Software Inc., San Jose, CA, USA). The ratio of the peak at 20° 2θ was the V-type relative crystallinity, while the relative crystallinity of A-type for maize starches or the B-type for potato
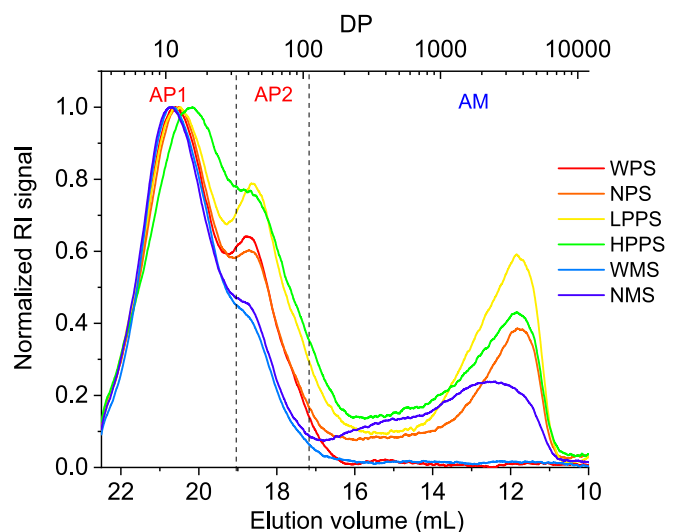
Fig. 2. Chain length distribution profiles of debranched starches determined by SEC (AP1, short amylopectin chains (DP 6–36); AP2: long amylopectin chains (DP 37–100); AM: amylose chains (DP 100–10,000); DP, degree of polymerization).

Fig. 3. Chain length distributions of debranched AP characterized by HPAEC-PAD. DP, degree of polymerization.

starches was calculated by the subtraction of V-type crystallinity from the total relative crystallinity.

2.8. Fourier Transform Infrared (FTIR) spectroscopy

The short-range order structure of the starch granules was estimated using a Bomem MB100 FTIR spectrometer (ABB-Bomem, Quebec, Canada) equipped with an attenuated total reflectance (ATR) single reflectance cell with a diamond crystal. The starch powder samples were scanned 64 times over the range of 4000–600 cm^{-1} at a resolution of 8 cm^{-1} against air. The ratio of absorbance at 1047 cm^{-1} to that at 1016 cm^{-1} was calculated as previously described (Wang, Wang, Guo, Liu, & Wang, 2017).

2.9. Scanning electron microscopy (SEM)

The granular morphology was analyzed using a Field Emission Scanning Electron Microscope (FE-SEM) (FEI Quanta 200). Starch samples were fixed, sputter-coated with gold, and images were taken at an acceleration voltage of 10 kV at 2000× magnification.

2.10. Statistical analysis

In the case of SAXS, ^{13}C NMR, and ^{1}H NMR, one measurement was performed, while other experiments were performed at least in triplicates, and the results were expressed as means ± standard deviations. Statistically significant differences ($p < 0.05$) were analyzed by Analysis

of Variance (ANOVA) followed by Duncan's test using SPSS 25.0 software (SPSS, Inc. Chicago, IL, USA). Normalized data were used to perform the principal component analysis (PCA) with the factoextra package in R (http://www.sthda.com/), and the mean values used for the correlation analysis. Flow diagram of the experimental design in this study is shown in Fig. 1.

3. Results and discussion

3.1. Effects of starch phosphate monoester on the glucan molecular structures

Chain length distribution (CLD) profiles (Fig. 2) of debranched starch samples examined by SEC showed three main components: short AP chains (AP1, DP 6–36), long AP chains (AP2, DP 37–100), and AM chains (DP > 100) (Zhong, Bertoft, Li, Blennow, & Liu, 2020). The peak positions, average chain lengths (ACLs), and relative contents (RCs) of these three starch components (Table 2) were analyzed to investigate the effects of the SPC on the structural features of debranched starches. The comparison between WPS and NPS, and between WMS and NMS in these structural parameters, demonstrated that increased AC resulted in a lower RC_{AP1} and RC_{AP2} in both maize and potato starch systems but had no effect on the ACLs of AP chains. The comparison of LPPS and HPPS showed that increased SPC was associated with increased $Peak_{AP1}$ and ACL_{AP1}, and decreased $Peak_{AP2}$ and ACL_{AM} in the potato starch system.

Detailed chain length distributions and fine structural parameters of AP molecules as determined by HPAEC-PAD (Zhong, Li, et al., 2021)

Table 2

Chain length distribution parameters of debranched starches analyzed by SEC.[a]

Starch varieties	$Peak_{AP1}$[b] (DP)	$Peak_{AP2}$ (DP)	$Peak_{AM}$ (DP)	ACL_{AP1} (DP)	ACL_{AP2} (DP)	ACL_{AM} (DP)	RC_{AP1} (%)	RC_{AP2} (%)	RC_{AM} (%)
WPS	12.4 ± 0.6[BCD]	40.6 ± 1.5[ABC]	n.d.[c]	14.6 ± 0.1[C]	58.1 ± 0.8[C]	n.d.	73.7 ± 0.7[B]	26.3 ± 0.7[A]	n.d.
NPS	12.7 ± 0.2[BC]	43.1 ± 1.5[AB]	3722 ± 6[A]	14.7 ± 0.1[BC]	63.1 ± 0.9[BC]	2181 ± 91[A]	56.0 ± 2.3[C]	21.4 ± 0.1[B]	22.6 ± 2.2[B]
LPPS	13.5 ± 0.1[B]	44.5 ± 2.2[A]	3710 ± 6[A]	15.0 ± 0.1[B]	68.8 ± 1.1[AB]	2083 ± 94[A]	44.1 ± 1.5[D]	24.7 ± 0.1[A]	31.2 ± 1.5[A]
HPPS	16.4 ± 0.5[A]	39.5 ± 3.1[BC]	3765 ± 78[A]	15.8 ± 0.1[A]	70.2 ± 1.6[A]	1807 ± 12[B]	46.4 ± 1.9[D]	26.5 ± 0.2[A]	27.1 ± 2.1[AB]
WMS	11.3 ± 0.8[D]	37.4 ± 0.4[C]	n.d.	14.1 ± 0.2[D]	57.4 ± 1.4[C]	n.d.	81.8 ± 0.2[A]	18.2 ± 0.2[C]	n.d.
NMS	11.9 ± 0.1[CD]	38.8 ± 1.0[BC]	2471 ± 507[B]	14.0 ± 0.1[D]	61.3 ± 5.7[C]	1494 ± 5[C]	60.0 ± 6.3[C]	15.4 ± 1.6[D]	24.0 ± 4.7[AB]

[a] Values are means ± SD. Values with different uppercase letters in the same column are significantly different at $p < 0.05$.

[b] CLD profiles (Fig. 2) of debranched starch contain three peaks: short AP (AP1, DP 6–36), long AP (AP2, DP 37–100) and AM chains (DP > 100). $Peak_X$: the DP of the peak of the fraction X; ACL_X: the average CL of the fraction X; RC_X: the relative content of the fraction X; DP, degree of polymerization.

[c] n.d. = not detectable.

Table 3
Chain length distribution parameters of debranched starches analyzed by HPAEC-PAD.[a]

Starch varieties	ACL_{fa} (DP)[b]	ACL_{fb1} (DP)	ACL_{fb2} (DP)	ACL_{fb3} (DP)	ACL_{all} (DP)	RC_{fa} (%)	RC_{fb1} (%)	RC_{fb2} (%)	RC_{fb3} (%)
WPS	10.1 ± 0.0^B	18.0 ± 0.0^B	29.5 ± 0.0^{AB}	53.2 ± 0.1^A	29.0 ± 0.3^{AB}	12.4 ± 0.2^{BC}	41.5 ± 0.9^{CD}	17.1 ± 0.4^B	28.5 ± 0.7^A
NPS	10.1 ± 0.1^B	18.1 ± 0.0^B	29.5 ± 0.1^{AB}	53.9 ± 0.1^A	29.2 ± 0.4^{AB}	11.7 ± 0.4^C	42.2 ± 1.2^C	17.5 ± 0.5^B	28.1 ± 1.0^A
LPPS	10.2 ± 0.1^B	18.0 ± 0.0^B	29.4 ± 0.2^B	53.6 ± 0.4^A	28.2 ± 0.5^B	13.3 ± 0.2^B	43.0 ± 0.2^{BC}	17.3 ± 1.0^B	26.1 ± 1.4^A
HPPS	10.1 ± 0.1^B	18.3 ± 0.0^A	29.7 ± 0.1^A	53.9 ± 0.4^A	30.2 ± 1.1^A	9.8 ± 0.5^D	38.8 ± 2.0^D	21.3 ± 0.2^A	29.2 ± 2.3^A
WMS	10.3 ± 0.0^A	17.9 ± 0.0^C	29.5 ± 0.1^{AB}	49.6 ± 0.2^B	25.2 ± 0.2^C	15.2 ± 0.2^A	45.8 ± 0.4^{AB}	18.6 ± 0.4^B	20.0 ± 0.2^B
NMS	10.3 ± 0.0^A	17.9 ± 0.0^C	29.5 ± 0.1^{AB}	48.9 ± 0.5^B	24.7 ± 0.7^C	16.0 ± 0.7^A	46.4 ± 1.8^A	18.1 ± 0.8^B	19.2 ± 1.6^B

[a] Values are means ± SD. Values with different uppercase letters in the same column are significantly different at $p < 0.05$.
[b] Amylopectin was divided into four fractions: *fa* (DP 6–12), fb_1 (DP 13–24), fb_2 (DP 25–36), and fb_3 (DP > 36) chains. ACL_X: the average CL of the fraction X; ACL_{all}: the average CL of the whole amylopectin; RC_X: the relative content of the fraction X; DP, degree of polymerization.

Table 4
α-1,6 ratio, the relative contents of double-helix (DH), single-helix (SH) and amorphous region (AR) derived from solid state NMR data, A/B/V type crystalline polymorphs derived from WAXS, and FTIR ratios of potato and maize starches.[a]

Starch varieties	α-1,6 ratio	NMR			WAXS				FTIR Ratio at 1047/1016 cm^{-1}
		DH (%)	SH (%)	AR (%)	A-type crystallinity (%)	B-type crystallinity (%)	V-type crystallinity (%)	Total crystallinity (%)	
WPS	6.3	34.0	n.d.[b]	66.0	n.d.	33 ± 1^B	2 ± 0^{BC}	35 ± 1^B	0.78 ± 0.04^A
NPS	4.0	30.4	1.6	68.0	n.d.	25 ± 0^D	1 ± 0^C	26 ± 1^D	0.73 ± 0.04^{AB}
LPPS	3.6	37.2	3.8	59.0	n.d.	38 ± 0^A	3 ± 0^A	41 ± 1^A	0.79 ± 0.02^A
HPPS	3.5	31.3	1.7	67.0	n.d.	28 ± 0^C	3 ± 1^{AB}	31 ± 1^C	0.70 ± 0.03^B
WMS	7.3	36.0	n.d.	64.0	34 ± 0^A	n.d.	1 ± 0^C	35 ± 0^B	0.74 ± 0.03^{AB}
NMS	5.2	31.1	3.9	65.0	28 ± 0^B	n.d.	2 ± 0^{BC}	30 ± 0^C	0.67 ± 0.01^B

[a] Values with different uppercase letters in the same column are significantly different at $p < 0.05$.
[b] n.d. = not detectable.

demonstrated that typical AP CLD profiles (Fig. 3 and Table 3) can be divided into four categories: fa (DP 6–12), fb_1 (DP 13–24), fb_2 (DP 25–36), and fb_3 (DP >36) chains (Hanashiro, Abe, & Hizukuri, 1996). The fa, fb_1, and fb_2 chains are mainly located in the crystalline nano-lamellae, while fb_3 chains have been suggested to be oriented in the amorphous nano-lamellae (Bertoft, 2017). Increasing AC in both potato (comparing WPS and NPS) and maize starch (comparing WMS and NMS) systems had no significant effect on the ACLs and RCs of the AP fraction. However, an elevated SPC in the potato starch systems with a similar AC level (comparing LPPS and HPPS) significantly increased the ACL_{fb1}, ACL_{fb2}, ACL_{all}, and RC_{fb2}, but decreased the RC_{fa} and RC_{fb1}, showing that higher SPC was related to more long AP chains with DP > 24 and less short AP chains with DP ≤ 24. GWD1 is reported to be highly active on long AP chains (DP ≥ 22) (Mikkelsen, Baunsgaard, & Blennow, 2004), and thus it is reasonable that more starch phosphate is generated in starches with high content of long AP chains during starch biosynthesis.

One-dimensional ^1H NMR spectra of potato and maize starches measured by ^1H NMR showed two main peaks (Fig. S1A) at 5.2 and 4.8 ppm, corresponding to the anomeric protons of α-1,4 and α-1,6 linkages, respectively (Bai, Shi, Herrera, & Prakash, 2011). The branching degree was calculated by the ratios of peak areas of α-1,6 to total peak areas of α-1,4 and α-1,6 linkages. It was found, as expected, that increased AC in both potato (comparing WPS and NPS) and maize starch systems (comparing WMS and NMS) was related to a decreased α-1,6 ratio (Table 4), as AM chains are mostly linear and with only a few branches. Similar α-1,6 ratio of HPPS (3.6) and LPPS (3.5) and amylose contents (Table 1, ~29 %) were found even though it is well documented that the AP in HPPS has longer chains (less branching, Table 3). As a consequence, the AM fraction in the LPPS must have somewhat fewer branches (more linear) than AM in the HPPS. AM is not normally considered to be phosphorylated, but the AM fraction of HPPS is probably so-called "amylose-like" material with relatively more branches than normal AM, which can be somewhat phosphorylated (Zhong, Qu, et al., 2022).
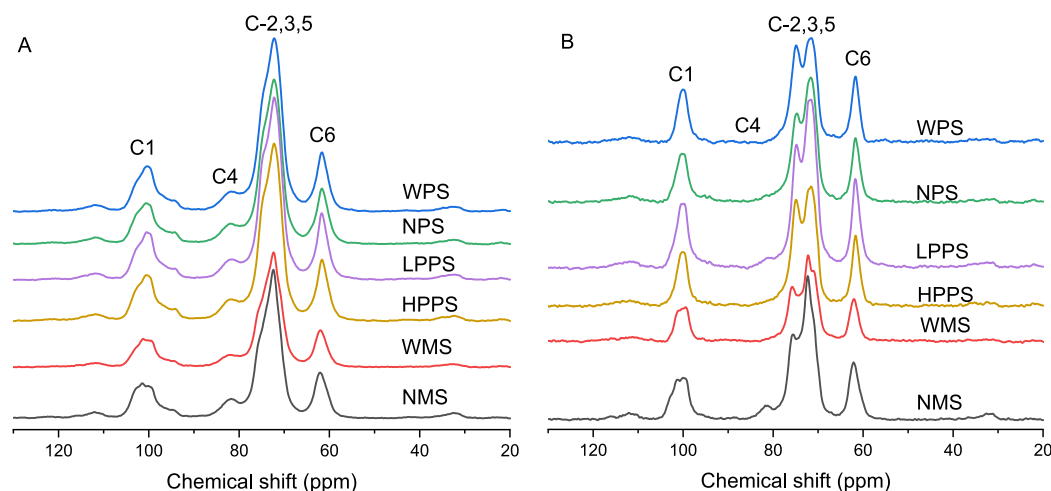
Fig. 4. The raw ^{13}C NMR spectra (A) and ordered sub-spectra (B) of starch samples.

Table 5
Nano-lamellar parameters of potato and maize starches as calculated from SAXS data.

Starch varieties	D (nm)[a]	I_{max} (a.u.)	d_a (nm)	d_c (nm)	d_{ac} (nm)
WPS	9.80	2170	2.94	6.88	9.82
NPS	10.09	2050	3.09	7.02	10.12
LPPS	9.89	2490	2.98	6.94	9.92
HPPS	10.12	851	3.02	7.10	10.12
WMS	9.96	1060	3.02	6.89	9.91
NMS	10.02	1550	3.06	6.96	10.02

[a] D: Bragg lamellar repeat distance; I_{max}: peak intensity; d_c: thickness of crystalline lamella; d_a: amorphous lamellae; d_{ac}: long period distance.

3.2. Effects of starch phosphate monoester on the helical structures

The helical structures, including the relative contents of single (SH), double helixes (DH), and amorphous regions (AR) analyzed by solid-state ^{13}C NMR (Fig. 4 and Table 4) showed that increased AC in both potato (comparing WPS and NPS) and maize starches (comparing WMS and NMS) decreased the relative DH content, and concomitant increased both SH and AR content. This is consistent with a previous study (Zhong, Li, et al., 2021). Amylose can form SH in the crystalline lamellae, which is interpreted as crystalline defects, whereas amylopectin side chains form ordered DH (Koroteeva et al., 2007). Interestingly, LPPS showed higher relative contents of DH and SH than HPPS, indicating that starch with lower SPC forms more DH and SH. This is likely attributed to the fact that phosphate monoesters exert a significant strain or induce local defects in the crystalline AP section to prevent helical formation (Hansen et al., 2009).

3.3. Effects of starch phosphate monoester on the crystalline and lamellar structures

WAXS profiles showed that all potato starches had a typical B-type allomorph characterized by major reflections at 2θ of 5.8° 15.0°, 16.9°, 22.1°, and 24.2° (Fig. S1B). The two maize starches had A-type allomorphs with strong reflections at 2θ of 15.2°, 17.2°, 18.2°, and 23.1°, consistent with previous data (Varatharajan et al., 2011; Zhong, Liu,

et al., 2020). The total relative crystallinities of the six starch types varied in different starch samples, from 26 % to 41 % (Table 4). Increasing AC in both potato (comparing WPS and NPS) and maize (comparing WMS and NMS) starch systems resulted in lower amounts of B-type and A-type crystals, respectively, due to the effect of AM on generating crystal defects (Bertoft, 2017). However, LPPS showed significantly higher B-type crystallinity than HPPS, corresponding to the higher relative contents of DH in LPPS, as mentioned in Section 3.2.

ATR-FTIR was used to investigate the structural ordering of the surface layer of the starch granules (Liu, Li, Li, Zhang, & Li, 2021). The deconvoluted ATR-FTIR spectra of the different starch samples (Fig. S1C), and the ratios of absorbance at 1047/1016 cm^{-1}, were calculated to indicate the degree of the short-range order structure related to molecular and rotational vibrations of the starch matrix (Table 4) (Cozzolino, Roumeliotis, & Eglinton, 2014; Liu et al., 2021; Van Soest, Tournois, de Wit, & Vliegenthart, 1995). Increasing AC in potato (comparing WPS and NPS) and maize (comparing WMS and NMS) starch systems, and enhancing SPC from LPPS to HPPS both resulted in lower 1047/1016 cm^{-1} ratios, suggesting that both AC and SPC had a disordering effect on the granular surfaces.

SAXS profiles (Fig. S2A) displayed the typical scattering peak around the q value of 0.06–0.07 Å^{-1}, demonstrating the presence of a 9–10 nm semi-crystalline lamellar structure in all starch samples. The 1D correlation function (Fig. S2B) was used to obtain the Bragg lamellar repeat distance (D), peak intensity (I_{max}), the thickness of crystalline lamella (d_c), the thickness of amorphous lamellar (d_a), and long period distance ($d_{ac} = d_c + d_a$) (Kuang et al., 2017), as shown in Table 5. Increasing AC in both maize starch (comparing WMS and NMS) and potato starch (comparing WPS and NPS) systems predominantly increased the d_c, d_a, D, and d_{ac}. Our previous study on rice starch also demonstrated that AC was positively correlated with both D and d_c (Zhong, Li, et al., 2021). In addition, HPPS showed higher d_c, d_a, D, and d_{ac} than those of LPPS, suggesting that phosphate groups may contribute to a more flexible lamellar structure. In addition, increased SPC (comparing LPPS and HPPS) reduced the I_{max} by as much as three-fold, indicating a disordering effect of phosphate monoesters on the lamellar structure.
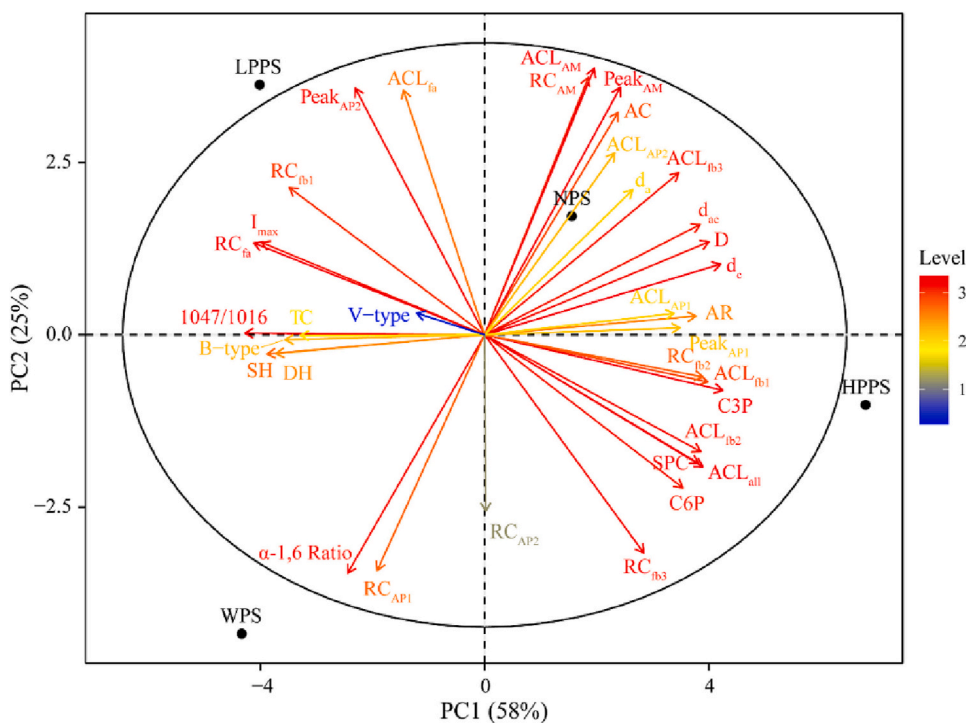
Fig. 5. Principal component analysis (PCA) of structural parameters of four potato starches. (SPC: starch phosphate content; C3P: C-3 phosphate monoester content; C6P: C-6 phosphate monoester content; AC: amylose content; Peak$_X$: the DP of the peak of the fraction X; ACL$_X$: average chain lengths (DP) of fraction X; RC$_X$: relative amount of fraction X; TC: total crystallinity; B-type: B-type crystalline polymorph; V-type: V-type crystalline polymorph; SH: relative amounts of single helices; DH: relative amounts of double helices; AR: relative contents of amorphous region; D: Bragg lamellar repeat distance; I_{max}: peak intensity; d_a: thickness of amorphous lamellae; d_c: thickness of crystalline lamellae; d_{ac}: long period distance).
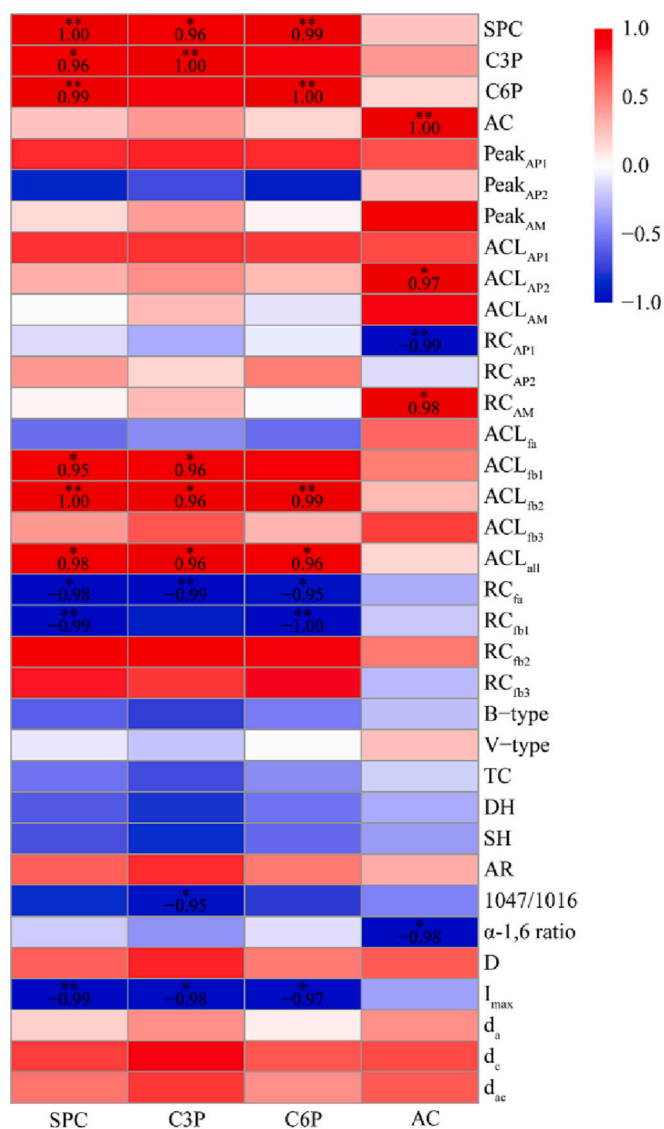
Fig. 6. Correlation analysis of structural parameters for four types of potato starches.
(All abbreviations are the same as in Fig. 5).

3.4. Effects of starch phosphate monoester on the granular structures

SEM images (Fig. S3) displayed ellipsoidal or round granules for all potato starches. Some irregular starch granules originated from the fusion of several smaller granules were observed for the HPPS; fusion is probably due to the high AC, as these granules have also been found in high amylose maize starches (Glaring, Koch, & Blennow, 2006). Nodular protrusions at the granular surface were found in a few granules of WPS, NPS and LPPS, likely indicating the irregular packing of the starch molecules in these regions (Blennow et al., 2003). The two types of maize starch showed either round or irregular shapes, which is in line with previous findings (Zhang et al., 2014).

3.5. Effects of starch phosphate monoesters on the multi-scale structures of potato starches — principal component analysis (PCA) and correlation analysis

Based on the above structural results, a higher AC is related to decreased double helical content, crystallinity and 1047/1016 cm^{-1} ratios, but increased d_c, d_a, D, and d_{ac} in both potato and maize systems, indicating that AC has similar effect in disordering crystalline and

lamellar structures of phosphorylated and non-phosphorylated starch systems. In addition, the effects of AC on the multi-scale structures of starch granules have already been widely documented (Kozlov et al., 2007; Li, Dhital, Gilbert, & Gidley, 2020; Zhong, Liu, et al., 2020), hence this part mainly discusses the effects of SPC and phosphate distributions on the starch structural traits using PCA and correlation analysis.

PCA analysis, where the two main principal components (PC1 and PC2) explained 83 % of the total variability, was conducted to interpret general effects of C6P, C3P, and SPC (Fig. 5). The four starches were grouped into four clusters, among which WPS was clustered with the α-1,6 ratio and relative content of AP1 chains (RC$_{AP1}$); NPS was clustered with average chain length of fb3 chains (ACL$_{fb3}$), ACL$_{AM}$, and Peak$_{AM}$; LPPS was grouped with high Peak$_{AP2}$, RC$_{fb1}$, and ACL$_{fa}$, and HPPS was characterized by having a high RC$_{fb2}$, ACL$_{fb1}$, and SPC/C3P/C6P. For phosphate monoesters, SPC and C6P were clustered together, consistent with previous results showing that C6P is the main component of phosphate groups in potato starches (Wikman et al., 2014; Wikman et al., 2011). Furthermore, the C6P was clustered with ACL$_{all}$ and ACL$_{fb2}$, whereas C3P was clustered with RC$_{fb2}$ and ACL$_{fb1}$ chains. The fb2 and fb1 AP chains function as the major and second connector chains, respectively, between the double helix and backbone of AP chains (Zhong, Bertoft, et al., 2020; Zhong, Li, et al., 2021). Hence, these data suggested that both C6P and C3P might be predominately located at the connector chains between the backbone and double helical matrix.

Consistent with the PCA results, correlation analysis (Fig. 6) showed that C3P and C6P were significantly positively correlated with ACL$_{fb2}$ and ACL$_{all}$, but negatively correlated with RC$_{fa}$. These results underpin that longer AP chains are highly suitable for accommodating phosphate groups, an effect attributed to the preferred catalytic activity of GWD1 and GWD3 on long AP chains (Mikkelsen et al., 2004). Phosphate monoesters might be preferably located far away from the branching points (normally more than nine glucosyl residues) (Wikman et al., 2011), and thus longer connectors are more likely to accommodate a higher number of phosphate monoesters. It is also worth mentioning that both C3P and C6P contents were negatively correlated with the scattering intensity (I_{max}), underlining the disordering effect of phosphate monoesters on lamellar structures, consistent with previous studies (Blennow & Engelsen, 2010; Kozlov et al., 2007). Interestingly, only the C3P content showed a significant negative correlation with the 1047/1016 cm^{-1} ratio as analyzed by FTIR, emphasizing the effect of C3P on disturbing the structures of starch granules in external regions, as also supported by force field models (Hansen et al., 2009). It was reported that phosphate groups exist in both the internal and external regions of potato starch granules (Glaring et al., 2006), and the present study emphasized that C3P might be mainly located in the external regions of starch granules. AC, one of the most important structural traits affecting the starch structure (Lin, Guo, Huang, et al., 2016; Lin, Guo, Zhao, et al., 2016; Zhong, Liu, et al., 2020), was also considered in the correlation analysis, and AC was found to be negatively correlated with RC$_{AP1}$ and the α-1,6 ratio, and positively correlated with ACL$_{AP2}$ and RC$_{AM}$, as shown in Fig. 6, consistent with previous reports (Cheetham & Tao, 1997; Zhong, Liu, et al., 2020). However, AC had no significant correlation with RC of fa, fb1, and fb2-three components of AP1, due to that RC$_{AP1}$ was calculated based on the total contents of AP and AM, while fa, fb1, and fb2 were calculated based on the total contents of only AP fraction. Compared to AC, SPC, C3P, and C6P had a stronger correlation with more structural parameters at molecular and lamellar structural levels, suggesting that SPC is an additional critical factor determining the structural traits of potato starches, even though its content is much lower than the AC.

3.6. Proposed schematic molecular structures of potato starches with different SPC and similar AC

As shown in Table 4, HPPS had a lower relative crystallinity, contents

LPPS

Crystalline lamella

Amorphous lamella

6.94 nm

2.98 nm

fa

fb1 fb2 fb1

fb3

HPPS

Crystalline lamella

Amorphous lamella

7.10 nm

3.02 nm

fa

fb1

fb1 fb2

fb3

● C-3 phosphate monoesters   ● C-6 phosphate monoesters
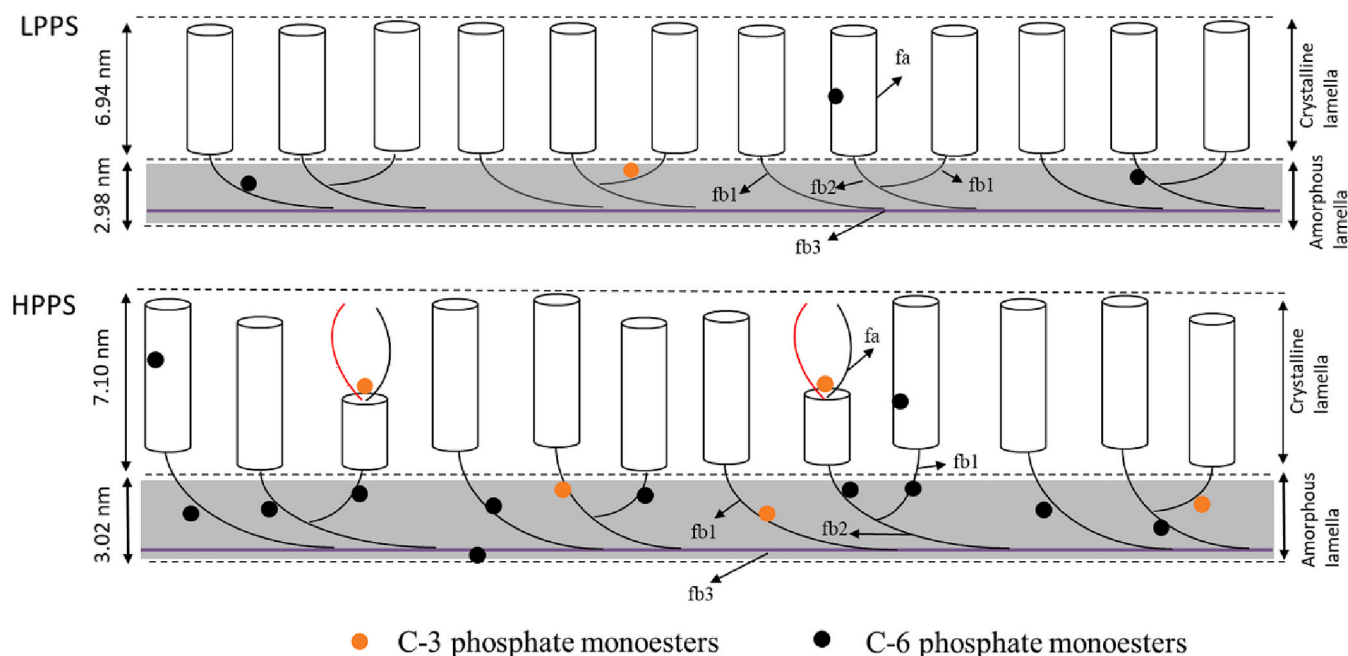
Fig. 7. Proposed schematic molecular structures of low phosphate potato starch (LPPS) and high phosphate potato starch (HPPS) (fa: amylopectin chains with DP 6–12; fb$_1$: amylopectin chains with DP 13–24); fb$_2$: amylopectin chains with DP 25–36; and fb$_3$: amylopectin chains with DP >36).

of single and double helices and I_{max} than LPPS, despite having a similar AC level (27.1 % cf. 31.2 % with no significant difference, Table 3). As a consequence, HPPS showed a more disordered matrix with crystal defects. This is probably attributed to its high SPC and/or long AP chains. For AP chains, the ACL$_{fb1}$ has a positive correlation with crystallinity and the relative content of the double helices in rice starches (Zhong, Li, et al., 2021). HPPS exhibited a significantly higher ACL$_{fb1}$, i.e., more chains involved in the formation of double helices and potentially in crystalline order. It was therefore expected that HPPS is more ordered than LPPS, however, this was not the case. Hence, the disordered structure of HPPS might have been attributed to its high SPC. As discussed in Section 3.5, both C3P and C6P are suggested to be mainly located at the connector chains between backbone chains and double helices (Blennow, Engelsen, Munck, & Møller, 2000). However, phosphorylation can also take place in double-helical segments at both the C-3 and C-6 positions, in which the C6P aligns well in the groove of the double helix, whereas C3P is more exposed and even strains the double helix by being incompatible with its conformation (Blennow & Engelsen, 2010; Hansen et al., 2009). A weak negative correlation between the C3P and double helix content (Fig. 6) further implies that C3P can induce local defects during the double helix formation (Blennow & Engelsen, 2010; Hansen et al., 2009). Therefore, we suggest that a high content of C3P was the main reason for the disordered structure of HPPS, probably by preventing the double helical formation and disorienting the parallel alignment of the double-helical lamellae, especially in the external regions of granules as shown by FTIR data (Table 4). Therefore, according to the above discussions based on our statistical results, previous work (Zhong, Liu, et al., 2020), literature (Blennow & Engelsen, 2010), and our current understanding within the area, schematic molecular structures of LPPS and HPPS are generated and presented in Fig. 7.

4. Conclusion

The effects of starch phosphate monoesters, namely C3P and C6P on the multi-scale structures of potato starches were studied using four types of potato starches with different SPC as models. The structural results suggest that a higher SPC is related to smaller amylopectin (AP) molecular size, more long AP chains with DP > 24 and fewer short AP chains with DP ≤ 24; moreover, higher SPC correlates with lower amounts of double helices and crystallinity, as well as higher long period distance, and a lower scattering intensity (I_{max}), indicating less structural ordering and a more flexible lamellar structure of potato starch with higher SPC. Correlation analysis suggested that C3P were significantly negatively correlated with I_{max} and short-range structural ordering at the starch granule surface (1047/1016 cm^{-1}), while C6P was only negatively correlated with the I_{max}. These results emphasized the disturbing effect of C3P on the structural ordering of potato starches, especially in the exterior part, probably by preventing the helical formation and disorienting the parallel alignment of the double-helical lamellae. This is the first study providing experimental data to support the functional differences of C3P and C6P in affecting the structural ordering of potato starches, and these findings will be helpful for potato breeding efforts that aim to control the phosphate group distributions to produce customized functional starch varieties. To support these efforts, future studies should provide a comprehensive understanding of how C3P, C6P or how the resulting structural differences caused by these starch phosphate monoesters affect the functionality of the potato starches.

CRediT authorship contribution statement

Li Ding: Conceptualization, Investigation, Methodology, Software, Writing – original draft. **Wenxin Liang:** Conceptualization, Investigation, Methodology, Software. **Jianzhou Qu:** Methodology, Software. **Staffan Persson:** Writing – review & editing. **Xingxun Liu:** Methodology, Software. **Klaus Herburger:** Methodology, Writing – review & editing. **Jacob Judas Kain Kirkensgaard:** Methodology, Writing – review & editing. **Bekzod Khakimov:** Methodology, Writing – review & editing. **Kasper Enemark-Rasmussen:** Methodology, Writing – review & editing. **Andreas Blennow:** Resources, Conceptualization, Supervision, Writing – review & editing. **Yuyue Zhong:** Resources, Conceptualization, Supervision, Writing – review & editing.

Declaration of competing interest

The authors declare that they have no known competing financial interests or personal relationships that could have appeared to influence the work reported in this paper.

Data availability

Data will be made available on request.

Acknowledgments

Appendix A. Supplementary data

Supplementary data to this article can be found online at https://doi.org/10.1016/j.carbpol.2023.120740.

References

Bai, Y., Shi, Y.-C., Herrera, A., & Prakash, O. (2011). Study of octenyl succinic anhydride-modified waxy maize starch by nuclear magnetic resonance spectroscopy. *Carbohydrate Polymers, 83*(2), 407–413.

Bertoft, E. (2017). Understanding starch structure: recent progress. *Agronomy, 7*(3), 56.

Blennow, A., Bay-Smidt, A. M., Olsen, C. E., & Møller, B. L. (2000). The distribution of covalently bound phosphate in the starch granule in relation to starch crystallinity. *International Journal of Biological Macromolecules, 27*(3), 211–218.

Blennow, A., Bay-Smidt, A. M., Wischmann, B., Olsen, C. E., & Møller, B. L. (1998). The degree of starch phosphorylation is related to the chain length distribution of the neutral and the phosphorylated chains of amylopectin. *Carbohydrate Research, 307* (1), 45–54.

Blennow, A., & Engelsen, S. B. (2010). Helix-breaking news: Fighting crystalline starch energy deposits in the cell. *Trends in Plant Science, 15*(4), 236–240.

Blennow, A., Engelsen, S. B., Munck, L., & Møller, B. L. (2000). Starch molecular structure and phosphorylation investigated by a combined chromatographic and chemometric approach. *Carbohydrate Polymers, 41*(2), 163–174.

Blennow, A., Hansen, M., Schulz, A., Jorgensen, K., Donald, A. M., & Sanderson, J. (2003). The molecular deposition of transgenically modified starch in the starch granule as imaged by functional microscopy. *Journal of Structure Biology, 143*(3), 229–241.

Blennow, A., Skryhan, K., Tanackovic, V., Krunic, S. L., Shaik, S. S., Andersen, M. S., & Nielsen, K. L. (2020). Non-GMO potato lines, synthesising increased-amylose and resistant starch, are mainly deficient in isoamylase debranching enzyme. *Plant Biotechnology Journal, 18*(10), 2096–2108.

Blennow, A., Wischmann, B., Houborg, K., Ahmt, T., Jorgensen, K., Engelsen, S. B., & Poulsen, P. (2005). Structure function relationships of transgenic starches with engineered phosphate substitution and starch branching. *Journal of Biological Macromolecules, 36*(3), 159–168.

Cai, C., Zhao, L., Huang, J., Chen, Y., & Wei, C. (2014). Morphology, structure and gelatinization properties of heterogeneous starch granules from high-amylose maize. *Carbohydrate Polymers, 102*, 606–614.

Carciofi, M., Blennow, A., Jensen, S. L., Shaik, S. S., Henriksen, A., Buléon, A., & Hebelstrup, K. H. J. B. P. B. (2012). Concerted suppression of all starch branching enzyme genes in barley produces amylose-only starch granules. *BMC Plant Biology, 12*(1), 223.

Cheetham, N. W. H., & Tao, L. (1997). The effects of amylose content on the molecular size of amylose, and on the distribution of amylopectin chain length in maize starches. *Carbohydrate Polymers, 33*(4), 251–261.

Cozzolino, D., Roumeliotis, S., & Eglinton, J. (2014). An attenuated total reflectance mid infrared (ATR-MIR) spectroscopy study of gelatinization in barley. *Carbohydrate Polymers, 108*, 266–271.

Engelsen, S. B., Madsen, A.Ø., Blennow, A., Motawia, M. S., Møller, B. L., & Larsen, S. (2003). The phosphorylation site in double helical amylopectin as investigated by a combined approach using chemical synthesis, crystallography and molecular modeling. *FEBS Letters, 541*(1–3), 137–144.

Glaring, M. A., Koch, C. B., & Blennow, A. (2006). Genotype-specific spatial distribution of starch molecules in the starch granule: A combined CLSM and SEM approach. *Biomacromolecules, 7*(8), 2310–2320.

Han, W., Zhang, B., Li, J., Zhao, S., Niu, M., Jia, C., & Xiong, S. (2017). Understanding the fine structure of intermediate materials of maize starches. *Food Chemistry, 233*, 450–456.

Hanashiro, I., Abe, J.-I., & Hizukuri, S. (1996). A periodic distribution of the chain length of amylopectin as revealed by high-performance anion-exchange chromatography. *Carbohydrate Research, 283*, 151–159.

Hansen, P. I., Spraul, M., Dvortsak, P., Larsen, F. H., Blennow, A., Motawia, M. S., & Engelsen, S. B. (2009). Starch phosphorylation–maltosidic restrains upon 3'- and 6'-phosphorylation investigated by chemical synthesis, molecular dynamics and NMR spectroscopy. *Biopolymers, 91*(3), 179–193.

Karlsson, M. E., Leeman, A. M., Björck, I. M. E., & Eliasson, A.-C. (2007). Some physical and nutritional characteristics of genetically modified potatoes varying in amylose/amylopectin ratios. *Food Chemistry, 100*(1), 136–146.

Koroteeva, D. A., Kiseleva, V. I., Sriroth, K., Piyachomkwan, K., Bertoft, E., Yuryev, P. V., & Yuryev, V. P. (2007). Structural and thermodynamic properties of rice starches with different genetic background part 1. Differentiation of amylopectin and amylose defects. *International Journal of Biological Macromolecules, 41*(4), 391–403.

Kozlov, S. S., Blennow, A., Krivandin, A. V., & Yuryev, V. P. (2007). Structural and thermodynamic properties of starches extracted from GBSS and GWD suppressed potato lines. *International Journal of Biological Macromolecules, 40*(5), 449–460.

Kuang, Q., Xu, J., Liang, Y., Xie, F., Tian, F., Zhou, S., & Liu, X. (2017). Lamellar structure change of waxy corn starch during gelatinization by time-resolved synchrotron SAXS. *Food Hydrocolloids, 62*, 43–48.

Li, C., Dhital, S., Gilbert, R. G., & Gidley, M. J. (2020). High-amylose wheat starch: Structural basis for water absorption and pasting properties. *Carbohydrate Polymers, 245*, Article 116557.

Li, H., Dhital, S., Flanagan, B. M., Mata, J., Gilbert, E. P., & Gidley, M. J. (2020). High-amylose wheat and maize starches have distinctly different granule organization and annealing behaviour: A key role for chain mobility. *Food Hydrocolloids, 105820*.

Lin, L., Guo, D., Huang, J., Zhang, X., Zhang, L., & Wei, C. (2016). Molecular structure and enzymatic hydrolysis properties of starches from high-amylose maize inbred lines and their hybrids. *Food Hydrocolloids, 58*, 246–254.

Lin, L., Guo, D., Zhao, L., Zhang, X., Wang, J., Zhang, F., & Wei, C. (2016). Comparative structure of starches from high-amylose maize inbred lines and their hybrids. *Food Hydrocolloids, 52*, 19–28.

Liu, C., Li, K., Li, X., Zhang, M., & Li, J. (2021). Formation and structural evolution of starch nanocrystals from waxy maize starch and waxy potato starch. *International Journal of Biological Macromolecules, 180*, 625–632.

Liu, Q., Tarn, R., Lynch, D., & Skjodt, N. (2007). Physicochemical properties of dry matter and starch from potatoes grown in Canada. *Food Chemistry, 105*(3), 897–907.

Mikkelsen, R., Baunsgaard, L., & Blennow, A. (2004). Functional characterization of alpha-glucan, water dikinase, the starch phosphorylating enzyme. *Biochemical Journal, 377*(2), 525–532.

Nayak, B., Berrios, D. J., & Tang, J. (2014). Impact of food processing on the glycemic index (GI) of potato products. *Food Research International, 56*, 35–46.

Noda, T., Kottearachchi, N. S., Tsuda, S., Mori, M., Takigawa, S., Matsuura-Endo, C., & Yamauchi, H. (2007). Starch phosphorus content in potato (Solanum tuberosum L.) cultivars and its effect on other starch properties. *Carbohydrate Polymers, 68*(4), 793–796.

Tan, I., Flanagan, B. M., Halley, P. J., Whittaker, A. K., & Gidley, M. J. (2007). A method for estimating the nature and relative proportions of amorphous, single, and double-helical components in starch granules by 13C CP/MAS NMR. *Biomacromolecules, 8* (3), 885–891.

Van Soest, J. J. G., Tournois, H., de Wit, D., & Vliegenthart, J. F. G. (1995). Short-range structure in (partially) crystalline potato starch determined with attenuated total reflectance Fourier-transform IR spectroscopy. *Carbohydrate Research, 279*, 201–214.

Varatharajan, V., Hoover, R., Li, J., Vasanthan, T., Nantanga, K. K. M., Seetharaman, K., & Chibbar, R. N. (2011). Impact of structural changes due to heat-moisture treatment at different temperatures on the susceptibility of normal and waxy potato starches towards hydrolysis by porcine pancreatic alpha amylase. *Food Research International, 44*(9), 2594–2606.

Viksø-Nielsen, A., Blennow, A., Jørgensen, K., Kristensen, K. H., Jensen, A., & Møller, B. L. (2001). Structural, physicochemical, and pasting properties of starches from potato plants with repressed r1-gene. *Biomacromolecules, 2*(3), 836–843.

Wang, S., Wang, S., Guo, P., Liu, L., & Wang, S. (2017). Multiscale structural changes of wheat and yam starches during cooking and their effect on in vitro enzymatic digestibility. *Journal of Agriculture and Food Chemistry, 65*(1), 156–166.

Wickramasinghe, H. A. M., Blennow, A., & Noda, T. (2009). Physico-chemical and degradative properties of in-planta re-structured potato starch. *Carbohydrate Polymers, 77*(1), 118–124.

Wikman, J., Blennow, A., & Bertoft, E. (2013). Effect of amylose deposition on potato tuber starch granule architecture and dynamics as studied by lintnerization. *Biopolymers, 99*(1), 73–83.

Wikman, J., Blennow, A., Buléon, A., Putaux, J.-L., Pérez, S., Seetharaman, K., & Bertoft, E. (2014). Influence of amylopectin structure and degree of phosphorylation on the molecular composition of potato starch lintners. *Biopolymers, 101*(3), 257–271.

Wikman, J., Larsen, F. H., Motawia, M. S., Blennow, A., & Bertoft, E. (2011). Phosphate esters in amylopectin clusters of potato tuber starch. *International Journal of Biological Macromolecules, 48*(4), 639–649.

Xu, J., Blennow, A., Li, X., Chen, L., & Liu, X. (2020). Gelatinization dynamics of starch in dependence of its lamellar structure, crystalline polymorphs and amylose content. *Carbohydrate Polymers, 229*, Article 115481.

Xu, X., Huang, X. F., Visser, R. G., & Trindade, L. M. (2017). Engineering potato starch with a higher phosphate content. *PLoS One, 12*(1), Article e0169610.

Zhang, B., Wang, K., Hasjim, J., Li, E., Flanagan, B. M., Gidley, M. J., & Dhital, S. (2014). Freeze-drying changes the structure and digestibility of B-polymorphic starches. *Journal of Agriculture and Food Chemistry, 62*(7), 1482–1491.

Zhong, Y., Bertoft, E., Li, Z., Blennow, A., & Liu, X. (2020). Amylopectin starch granule lamellar structure as deduced from unit chain length data. *Food Hydrocolloids, 108*, Article 106053.

Zhong, Y., Keeratiburana, T., Kain Kirkensgaard, J. J., Khakimov, B., Blennow, A., & Hansen, A. R. (2021). Generation of short-chained granular corn starch by maltogenic alpha-amylase and transglucosidase treatment. *Carbohydrate Polymers, 251*, Article 117056.

Zhong, Y., Li, Z., Qu, J., Bertoft, E., Li, M., Zhu, F., & Liu, X. (2021). Relationship between molecular structure and lamellar and crystalline structure of rice starch. *Carbohydrate Polymers, 258*, Article 117616.

Zhong, Y., Liu, L., Qu, J., Blennow, A., Hansen, A. R., Wu, Y., & Liu, X. (2020). Amylose content and specific fine structures affect lamellar structure and digestibility of maize starches. *Food Hydrocolloids, 108*, Article 105994.

Zhong, Y., Qu, J. Z., Liu, X., Ding, L., Liu, Y., Bertoft, E., & Blennow, A. (2022). Different genetic strategies to generate high amylose starch mutants by engineering the starch biosynthetic pathways. *Carbohydrate Polymers, 287*, Article 119327.

Zhong, Y., Tian, Y., Liu, X., Ding, L., Kirkensgaard, J. J. K., Hebelstrup, K., & Blennow, A. (2021). Influence of microwave treatment on the structure and functionality of pure amylose and amylopectin systems. *Food Hydrocolloids, 119*, Article 106856.

Zhou, W., Yang, J., Hong, Y., Liu, G., Zheng, J., Gu, Z., & Zhang, P. (2015). Impact of amylose content on starch physicochemical properties in transgenic sweet potato. *Carbohydrate Polymers, 122*, 417–427.